Asian Journal of Chemistry; Vol. 26, No. 5 (2014), 1363-1366

ASIAN JOURNAL OF CHEMISTRY

http://dx.doi.org/10.14233/ajchem.2014.17232

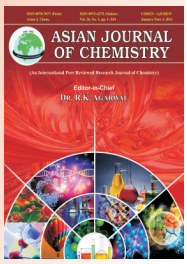

One-Step Solvothermal Synthesis Flower-like $CuInS_2$ and Application in Dye-Sensitized Solar Cells as Counter Electrode†

L. ZHOU[1], X. YANG[1], A.L. FENG[1], H.B. TANG[1], Z.L. DING[1], Y.Q. MA[1], M.Z. WU[1], S.W. JIN[1] and G. LI[1,2,*]

[1]School of Physics and Materials Science, Anhui University, Hefei 230601, P.R. China
[2]Anhui Key Laboratory of Information Materials and Devices, Hefei 230601, P.R. China

*Corresponding author: Fax: +86 551 63861992; Tel: +86 551 63861867; E-mail: liguang1971@ahu.edu.cn

Published online: 1 March 2014; AJC-14773

Chalcopyrite flower-like $CuInS_2$ were successfully synthesized by a one-step solvothermal method and has been applied as a counter electrode for efficient dye-sensitized solar cells. The as-synthesized flower-like $CuInS_2$ were composed of nanoplates. The prepared $CuInS_2$ powders occupy energy band gaps of 1.38 eV, which is considerably approaching to ideal band gap for optimum solar energy conversion *via* the photovoltaic effect. The dye-sensitized solar cells with flower-like $CuInS_2$ as a counter electrode can yield 4.5 % photoelectric conversion efficiency.

Keywords: $CuInS_2$, Solvothermal, Counter electrode, Dye-sensitized solar cells.

INTRODUCTION

The dye-sensitized solar cells (DSSC) has been considered as an ideal alternative of silicon-based solar cells despite the low conversion efficiency compared to single crystal Si solar cells since it was proposed in 1991 by Prof. Michael Grätzel[1-3]. Low cost, long life, easy to manufacture and other advantages compared with conventional solar cells prompt it to prosperity[4]. $CuInS_2$ as a typical ternary I-II-IV_2 compounds semiconductor material attracts a good proportion of research attention because of its high absorption coefficient, good stability under solar radiation, easy conversion of n/p carrier type and band gap of 1.45 eV, which is close to the optimum range for high photovoltaic conversion[5,6].

It is well known that the platinum metal is used as counter electrode in the traditional dye-sensitized solar cells due to its high catalytic activity. However, noble metal Pt is relatively so expensive to restrict its large-scale manufacture[7]. Hence, searching for low cost substitutes for Pt as active materials for counter electrode become the focus of the current work. $CuInS_2$ as a substitute has been attracted a lot of attention and different morphologies of $CuInS_2$ have been obtained, such as nanoparticles[8-10], foam-like nano-crydtallites[11], nano-wires[12,13], microspheres[14-16], vertically oriented nanosheeets[7] and bullet-like nanocrystals[17]. Here, we report the synthesis of flower-like $CuInS_2$ by a one-step solvothermal method and apply as counter electrodes in dye-sensitized solar cells. This morphology has some obvious advantages, *e.g.*, large specific surface area to adsorb more electrolyte. Using this prepared material, a higher photoelectric conversion effciency has been exhibited.

EXPERIMENTAL

Cuprous chloride, indium chloride tetrahydrate, sublimed sulfur powder were used as received without further purification.

Synthesis of flower-like $CuInS_2$ microarchitectures: In a typical synthesis[18,19], CuCl (1.0 mmol) and $InCl_3{\cdot}4H_2O$ (1.0 mmol) and sublimed sulfur powders (3.0 mmol) were dispersed in 35 mL of triethylene glycol with the aid of thoroughly magnetic stirring and then followed by ultrasonication for 20 min to obtain an opaque yellow-green suspension. Subsequently, the suspension was transferred into a 50 mL Teflon-lined stainless steel autoclave. The autoclave was sealed and maintained at 200 ºC for 48 h. After cooling to room temperature naturally, the obtained black precipitate was filtered off, washed with absolute ethanol and distilled water for several times and finally dried in a vacuum at 60 ºC for 12 h to obtain high-purity $CuInS_2$.

Preparation of counter electrodes (CEs): A $CuInS_2$ counter electrode was typically prepared by dispersing $CuInS_2$

†Presented at The 7th International Conference on Multi-functional Materials and Applications, held on 22-24 November 2013, Anhui University of Science & Technology, Huainan, Anhui Province, P.R. China

powder (0.1 g) and polyethylene glycol powder (0.025 g) in 1 mL absolute ethanol and then ground with an agate mortar to form a colloid. Afterwards, the colloid was coated on the FTO conductive glass *via* the doctor-blading technique followed by drying naturally and annealing at 550 ºC for 0.5 h under the protection of nitrogen. Then it was prepared after naturally cooling to room temperature.

Fabrication of dye-sensitized solar cells: The prepared photoanodes were porous TiO_2 film fabricated with commercial TiO_2 slurry (Wuhan Georgi Science Instrument Co., Ltd., China) by the doctor-blading technique and sensitized with N719 dye. Subsequently, the photoanodes were assembled with the as-prepared counter electrodes. The electrolyte contains 0.5 M LiI, 0.6 M 1-propy1-2,3-dimethylimidazolium iodide, 0.05 M I_2 and 0.5 M 4-*tert*-buylpyridine with acetonitrile as the solvent was then injected.

The as-synthesized samples were characterized by X-ray powder diffraction (XRD) equipped with monochromatized CuK_α radition (λ = 1.5406 Å) at 36 KV and 25 mA. Scanning electron microscopy (SEM) images were acquired using a Hitachi S-4800 scanning electron microscope. Transmission electron microscopy (TEM) images were carried out on a JEOL JEM-100SX transmission electron microscope at an acceleration voltage of 200KV. The UV-visible spectra were recorded on a liquid Hitachi U-4100 Spectrophotometer. The J-V curves were determined using a xenon lamp solar simulator under AM 1.5 illumination (Continuous Solar Simulator for PV Cells) and measured under 100 mW cm^{-2} which was calibrated beforehand by an optical power meter. All the measurements were performed at room temperature.

RESULTS AND DISCUSSION

Flower-like $CuInS_2$ were successfully synthesized *via* a facile solvothermal method at 200 ºC for 48 h. XRD patterns shown in Fig. 1 easily give the phase and crystallinity of the as-synthesized products. The XRD patterns are indexed to chalcopyrite crystal structure and all the diffraction peaks can match well with the reported data of tetragonal lattice parameters of a = 5.529 Å and c = 11.11 Å (JCPDS card No. 27-0159, a = 5.523 Å, c = 11.14 Å). No miscellaneous characteristic peaks such as CuS or In_2S_3 were detected, which indicates that a high purity $CuInS_2$ phase has been obtained.

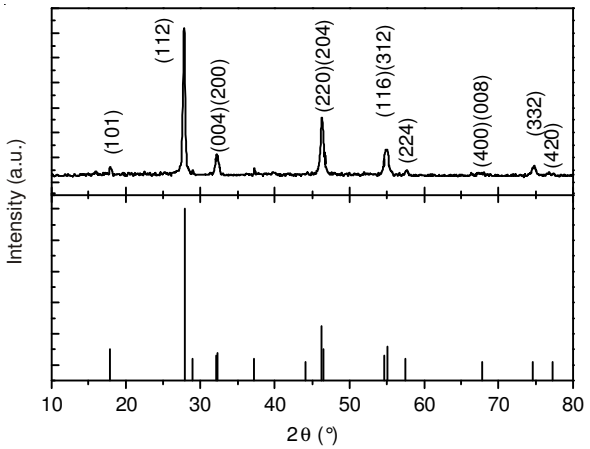

Fig. 1. XRD patterns of flower like $CuInS_2$ and the standard card of JCPDS No. 27-0159

The morphology of $CuInS_2$ was clearly demonstrated in Fig. 2. SEM images reveal that the sample is mainly composed of mono-dispersed microspheres with average diameter of 5 μm. In Fig. 2, a single $CuInS_2$ hierarchical microsphere which was composed of many interleaving two-dimensional flakes (average thickness 26 nm) cause the formation of irregular cavities with different sizes inside the microsphere was observed. Further structural analysis was performed by the TEM images shown in Fig. 3.

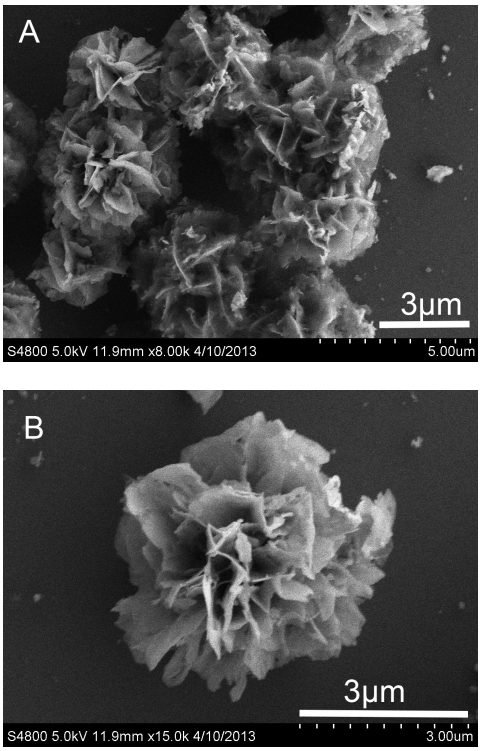

Fig. 2. SEM images of flower like $CuInS_2$ at different magnifications

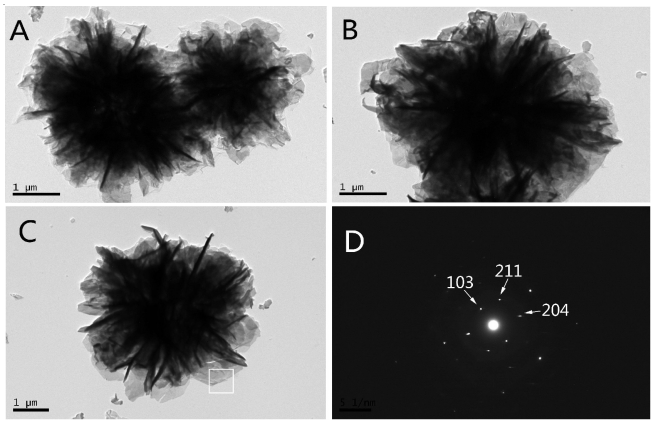

Fig. 3. TEM images (A, B and C) of flower like CuInS2 at different magnifications and the corresponding SAED image (D), the selected area was marked in C of Fig. 3

The flower-like microspheres display pale edges and dark centers which suggest the existence of side/density variations intrinsic inside the spheres[20]. The selected area electron diffraction (SAED) pattern of a portion of the flakes ultrasonically exfoliated from a microsphere exhibits that the flakes are single crystals with a tetragonal lattice, which was shown in Fig. 3D.

The UV-visible absorption spectra shown in Fig. 4 provide the optical properties of the as-synthesized sample. It clearly indicates that the sample exhibits a abroad peak at around 720 nm, which illustrates that the obtained sample's photo absorption range mostly distribute in the visible light region and a slight blue-shift phenomenon compared with the bulk $CuInS_2$ (at 810 nm). The curve of $(\alpha h\nu)^2$ *versus* photon energy was also drawn in Fig. 4. The value of the band gap of the as-synthesized $CuInS_2$ microsphere can be intuitively observed as 1.38 eV in the figure through the intersection point of the extrapolated linear portion and the abscissa, which is near to the previous reported value of bulk $CuInS_2$ (1.53 eV). It is well known that the band structure of a semiconductor is strongly dependent on the pattern of orbital interactions, which is affected by the symmetry and the microstructure of the crystal[21]. The result is in accordance with the theoretical calculation that disordering of cations in chalcopyrite structure induces band gap decrease, which has been reported in previous literatures[22-24]. The different band gaps of bulk and nanoscale $CuInS_2$ are presumably associated with crystal structure. In the previous literature[4], the energy gap alters followed by variation of the [Cu]/[In] and[S]/[In] ratio, which indicates that many factors probably lead to the decrease of band gap of nanoscale $CuInS_2$ compared to bulk $CuInS_2$. In this regard, the flower-like $CuInS_2$ microsphere can be a suitable catalytic material for the dye-sensitized solar cells.

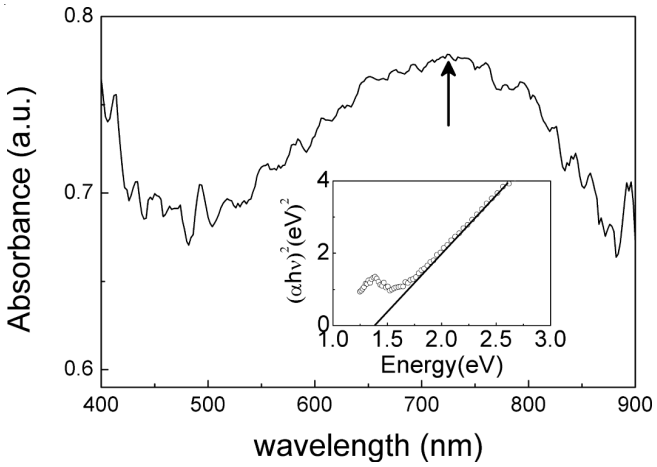

Fig. 4. The UV-visible absorption spectra of the as-prepared $CuInS_2$ sample and the bandgap value which was estimated by a related curve of $(\alpha h\nu)^2$ *versus* photon energy plotted

The capability of the dye-sensitized solar cells was investigated and shown in Fig. 5. The flower-like $CuInS_2$ nanostructure has higher electrocatalytic activity because of its larger specific surface area to capture more electronics and provide more transport channels compared to other morphology nanostructure. Fig. 5(a) shows the photocurrent *versus* voltage curve, which indicates that the short current density J_{sc} was about 11.5 mA cm^{-2} and the open voltage was 0.71 V. Through the curve, we can calculate the filling factor (FF) = 55.5 % of the dye-sensitized solar cells and the photoelectric conversion efficiency can yield 4.5 % [Fig. 5(b)]. It can be seen that filling factor of the dye-sensitized solar cells is not high. The filling factor may reflect the output characteristics of solar cells, which

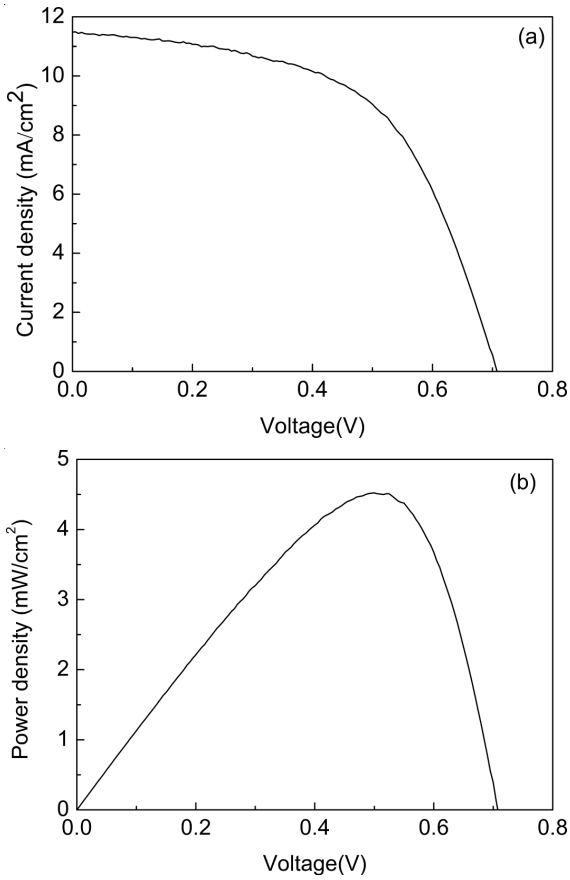

Fig. 5. J-V curve (a) and P-V curve (b)of the dye-sensitized solar cellss with flower like $CuInS_2$ as counter electrode under AM 1.5 solar simulator illumination at 100 mW cm^{-2}

is an important parameter. There are many factors to affect the filling factor including series resistance and parallel resistance of solar cells. The greater solar cell series resistance and the smaller solar cell parallel resistance are, the smaller the filling factor is. The filling factor is also related to the internal resistance, which indicates that the greater the internal resistance is, the smaller the filling factor is. According to chemical analysis, internal resistance also restricts mass transfer kinetics of electrolyte, namely the redox couple's diffusion rate of the electrolyte. The fill factor is facile to be affected by the interface of TiO_2 photo anode and electrolyte. The reflux of conductive electrons back into the the electrolyte result in the decrease of filling factor. This explains the filling factor is not so high and we can proceed to reduce series resistance, increase parallel resistance and reduce internal resistance to increase the filling factor. Generally, the higher filling factor can promote the photoelectric conversion efficiency parameter. If filling factor is enhanced to more than 65 %, the much higher conversion efficiency will be expected.

EIS measurements were tested on dummy cells with a typical sandwich-like structure, *i.e.*, two symmetric counter electrode and the electrolytes between the two electrodes. The Nyquist plots (A) were shown in Fig. 6, which corresponds with the equivalent circuit diagram of the impedance (B). In the figure, a typical semicircle is visible[25]. Generally, the intercept on the real axis (Z'-axis) of the high-frequency region can be assigned to the series resistance (R_s). The value of series

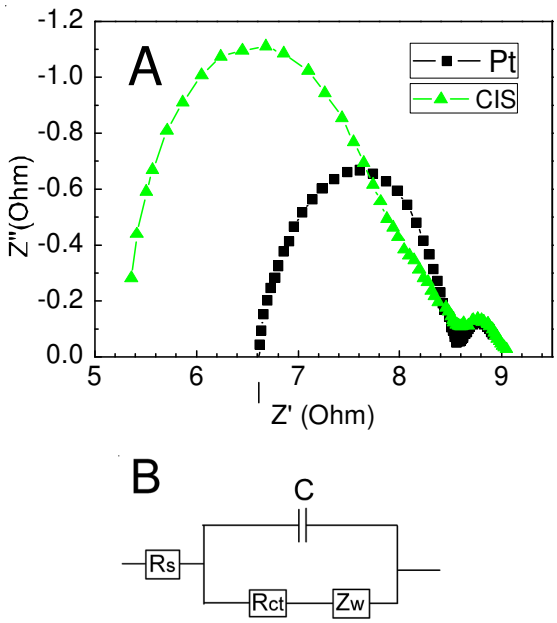

Fig. 6. Nyquist plots of EIS for the symmetrical cells fabricated with $CuInS_2$ film and sputtering Pt, respectively (with areas of 0.25 cm^2) (A) and the fitting equivalent circuit (B)

resistance is 5.562 Ω, which is smaller than the value of Pt electrode. In literature[26], when the two devices have the same photocurrent, the higher series resistance leads to higher photovoltage, which indicates that the V_{oc} of obtained $CuInS_2$ is lower than the Pt. The size of the first semicircle (on the left) is consistent with charge-transfer (R_{ct}) between the electrode and electrolyte and the double-layer capacitance (C) at the electrolyte-counter electrode interface. The results of data analysis from the EIS spectra are summarized in Table-1. It was generally recognized that a smaller Rct represents a higher electrocatalytic activity[27,28]. Charge transfer of $CuInS_2$ electrode possesses a larger value (2.842 Ω) than the Pt electrode (1.734 Ω). Charge transfer is associated with the power conversion efficiency and the decrease of the charge-transfer resistance leads to the improvement of the energy conversion efficiency, which is consistent with our experimental results.

TABLE-1
EIS PARAMETERS OF THE DUMMY CELL ASSEMBLED WITH TWO IDENTICAL COUNTER ELECTRODES OF $CuInS_2$ AND Pt

CE	R_s (Ω)	R_{ct} (Ω)	C (μF)	Zw (Ω)
$CuInS_2$	5.562	2.842	5.923	1.596
Pt	6.767	1.734	47.77	2.625

Conclusion

The flower-like $CuInS_2$ were successfully synthesized *via* a facile one-step solvothermal reaction and the $CuInS_2$ counter electrodes for dye-sensitized solar cellss were prepared by doctor-blading technique. The J-V curves indicated that flower-like $CuInS_2$ could greatly promote the reduction of I_3^- and the photoelectric conversion efficiency of dye-sensitized solar cellss with prepared counter electrodes reached 4.5 %. As a promising alternative to Pt electrode, $CuInS_2$ nanomaterials may have a good development prospect.

ACKNOWLEDGEMENTS

This work was financially supported by National Natural Science Foundation of China (11174002) and by '211 Project' of Anhui University.

REFERENCES

1. W.U. Huynh, J.J. Dittmer and A.P. Alivisatos, *Science*, **295**, 2425 (2002).
2. M. Grätzel, U. Bach, D. Lupo, P. Comte, J.E. Moser, F. Weissörtel, J. Salbeck and H. Spreitzer, *Nature*, **395**, 583 (1998).
3. M. Gratzel, *Nature*, **414**, 338 (2001).
4. R. Fan, D.C. Kim, S.H. Jung, J.H. Um, W. In Lee and C.W. Chung, *Thin Solid Films*, **521**, 123 (2012).
5. J.L. Shay and J.H. Wernick, Ternary Chalcopyrite Semiconductors: Growth, Electronic Properties and Applications, Pergamon, New York, edn 1 (1975).
6. K. Ernst, A. Belaidi and R.K nenkamp, *Semicond. Sci. Technol*., **18**, 475 (2003).
7. J. Yang, C.X. Bao, J.Y. Zhang, T. Yu, H. Huang, Y.L. Wei, H. Gao, G. Fu, J.G. Liu and Z.G. Zou, *Chem. Commun.*, **49**, 2028 (2013).
8. D.P. Dutta and G. Sharma, *Mater. Lett*., **6**, 2395 (2006).
9. S.L. Castro, S.G. Bailey, R.P. Raffaelle, K.K. Banger and A.F. Hepp, *Chem. Mater*., **15**, 3142 (2003).
10. Q.Y. Lu, J.Q. Hu, K.B. Tang, Y.T. Qian, G.E. Zhou and X.M. Liu, *Inorg. Chem*., **39**, 1606 (2000).
11. G.Z. Shen, D. Chen, K.B. Tang, Z. Fang, J. Sheng and Y.T. Qian, *J. Cryst. Growth*, **254**, 75 (2003).
12. K. Wakita, M. Iwai, Y. Miyoshi, H. Fujibuchi and A. Ashida, *Compos. Sci. Technol*., **65**, 765 (2005).
13. K.B. Tang, Y.T. Qian, J.H. Zeng and X.G. Yang, *Adv. Mater*., **15**, 448 (2003).
14. J.C. Zhou, S.W. Li, X.L. Gong, Y.L. Yang and Y. Guo, *Mater. Lett*., **65**, 2001 (2011).
15. H.M. Hu, B.J. Yang, X.Y. Liu, R. Zhang and Y.T. Qian, *Inorg. Chem. Commun*., **7**, 563 (2004).
16. X.L. Gou, S.J. Peng, L. Zhang, Y.H. Shi, J. Chen and P.W. Shen, *Chem. Lett*., **35**, 1050 (2006).
17. J. Guo, W.H. Zhou, M. Li, Z. Hou, J. Jiao, Z.J. Zhou and S.X. Wu, *J. Cryst. Growth*, **359**, 72 (2012).
18. L. Zheng, Y. Xu, Y. Song, C.Z. Wu, M. Zhang and Y. Xie, *Inorg. Chem*., **48**, 4003 (2009).
19. F. Aslan, M.Z. Zarbali, B. Yesilata and I.H. Mutlu, *Mater. Sci. Semicond. Process*., **16**, 138 (2013).
20. Y.X. Qi, K.B. Tang, S.Y. Zeng and W.W. Zhou, *Microporous Mesoporous Mater*., **114**, 395 (2008).
21. Y.X. Qi, Q.C. Liu, K.B. Tang, Z.H. Liang, Z.B. Ren and X.M. Liu, *J. Phys. Chem. C*, **113**, 3939 (2009).
22. A. Zunger, *Appl. Phys. Lett*., **50**, 164 (1987).
23. C. Rinc'n, *Phys. Rev. B*, **45**, 12716 (1992).
24. S.H. Wei, L.G. Ferreira and A. Zunger, *Phys. Rev. B*, **45**, 2533 (1992).
25. J.D. Roy-Mayhew, D.J. Bozym, C. Punckt and I.A. Aksay, *ACS Nano*, **4**, 6203 (2010).
26. L.X. Yi, Y.Y. Liu, N.L. Yang, Z.Y. Tang, H.J. Zhao, G.H. Ma, Z.G. Su and D. Wang, *Energy Environ. Sci*., **6**, 835 (2013).
27. M.X. Wu, X. Lin, A. Hagfeldt and T.L. Ma, *Angew. Chem. Int. Ed*., **50**, 3520 (2011).
28. Z.Y. Zhang, X.Y. Zhang, H.X. Xu, Z.H. Liu, S.P. Pang, X.H. Zhou, S.M. Dong, X. Chen and G.L. Cui, *ACS Appl. Mater. Interfaces*, **4**, 6242 (2012).